Apparent Hysteresis in a Driven System with Self-Organized Drag

Mikko Haataja,[1,*] David J. Srolovitz,[1] and Ioannis G. Kevrekidis[2]

[1]*Princeton Materials Institute and Department of Mechanical and Aerospace Engineering, Princeton University, Princeton, New Jersey 08544, USA*

[2]*Department of Chemical Engineering, PACM and Mathematics, Princeton University, Princeton, New Jersey 08544, USA*

(Received 28 October 2003; published 23 April 2004)

The motion of extended defects in materials is often resisted by interaction with diffusing impurities. The defect undergoes a transition from slow to fast migration, or vice versa. This transition is commonly hysteretic, with the defect jumping back and forth between these kinetic states. We explore such hysteresis within a kinetic Monte Carlo simulation. After identifying the slow variables, we construct an effective potential that quantitatively describes the stable and metastable states of the system (a bifurcation diagram) and the kinetics of the transitions between these. This description provides a means to determine whether hysteresis will be observed in a particular simulation and the detailed nature of this hysteresis (switching times).

DOI: 10.1103/PhysRevLett.92.160603 PACS numbers: 05.10.Gg, 61.72.–y

Driving an extended defect or domain wall in a system that contains stationary or mobile impurities with which the domain wall interacts lies at the heart of many physical phenomena, including the motion of grain boundaries in polycrystalline materials [1], the motion of vortex lines in dirty superconductors [2,3], driven charge-density waves [4], the motion of dislocations in impure metals undergoing plastic deformation (i.e., Portevin-LeChatelier effect [5]), ferroelectric domain wall dynamics [6], and stick-slip phenomena in tribology [7]. The self-organization of the impurities through segregation to these extended defects (i.e., the source of drag) commonly leads to strikingly nonlinear behavior. The ability to quantitatively model such systems holds the key to designing a wide range of devices and optimizing their operating conditions. While understanding the transition between the slow and fast kinetic regimes is vital, the dynamics become particularly difficult to characterize in the neighborhood of such a transition (neutral stability).

When equations that describe the macroscopic behavior of a system are known analytically, an established set of mathematical or computational tools is available for analyzing the dynamics (e.g., locating and characterizing transitions). Many "real world" applications are too complex to characterize in terms of simple equations. Microscopic simulations are becoming an increasingly common approach to analyze situations where such macroscopic models are not available analytically. This is the case for driving a domain wall through a field of mobile impurities: although analytical models exist, they do not accurately and/or fully predict the range of observed behavior. In such systems, there is a "specter" of hysteresis in the transition from slow to fast motion—sometimes it is seen [8] and sometimes not [9]. Classical theories of such phenomena [1] are usually one dimensional and show that the domain wall velocity vs driving force curve can be multivalued, i.e., suggest the existence of hysteresis. In this Letter, we examine this phenomenology—try to understand its roots and argue that it is both the physics *and* the observer that determines whether hysteresis will appear in experiments or simulations.

We illustrate the issues arising in considering hysteresis within the context of the classical solute drag effect, in which diffusing impurities interact with a migrating domain wall and impede its motion. In particular, we employ a variant of the Ising model in which the domain wall moves under the influence of an external field, and interstitial impurities diffuse and are attracted to the domain wall [9]. The energy of the model system is $\mathcal{H}/k_BT = -J/2\sum s_i s_j - h\sum s_i + E_0/4\sum \epsilon_\alpha |\sum s_j|$, where $s_i = 1$ in one domain and -1 in the other, ϵ_α is zero or 1 depending on whether an impurity occupies interstitial site α or not, $E_0 > 0$ implies that the impurities are attracted to the interface, and $J > 0$ and h scale the domain wall energy and the driving force, respectively. The first term represents the total energy of domain walls in the pure system, the second term accounts for the external drive, and the last term describes the interaction between the impurities and the domain wall. The parameters chosen for the present study were $J = 2.0$ and $E_0 = [4.0, 7.0]$ and the bulk impurity concentration was set to 1% ($c_{\text{imp}} = 0.01$).

Initially, the 2D computational domain contains a single, straight domain wall and randomly placed interstitial impurities. The system evolves by randomly choosing spins to flip or impurities to exchange with neighboring empty sites, with probability proportional to their relative density and the impurity diffusivity m, as described by Mendelev *et al.* [9]. An attempted change is accepted if it lowers the energy of the system ($\Delta\mathcal{H} \leq 0$) or, if $\Delta\mathcal{H} > 0$, it is accepted provided that $e^{-\Delta\mathcal{H}/k_BT} < R$, where R is a random number uniformly distributed between 0 and 1. The simulation clock

advances by one unit when all of the spins have been sampled once, on average. When the domain wall gets close to one end of the simulation cell, more sites are added to that end and removed from the opposite end, thereby making the length of the system L effectively infinite [9]. The results presented below are for a relatively small simulation cell width ($W = 32$). This was done to prevent excessive domain wall roughening, which tends to smear the slow-fast domain wall transition. The effect of system size is very important for the observation of hysteresis but will be the subject of a future report.

The domain wall velocity results from a balance between the external field, which controls the propagation velocity in the pure system, and the diffusing impurities, which locally impede domain wall migration. In the limit of large drive and weak domain wall-impurity interactions, the impurities have little influence on the domain wall motion. Conversely, decreasing the drive and increasing the attraction of the impurities to the domain wall E_0 leads to very slow domain wall dynamics, due to the strong segregation of the impurities onto the domain wall. However, as is demonstrated below, the drive, impurity-domain wall interaction, impurity mobility, and the average impurity concentration may conspire to give rise to an intermediate regime: a regime where the domain wall is captured by the impurities, then escapes and travels nearly unimpeded until it is recaptured. This is the "jerky" (stick-slip-like) domain wall motion regime, where hysteresis may be observed.

Figure 1 shows the mean domain wall position R vs time t for $h = 0.12$ and several values of the domain wall/impurity interaction strength E_0. These curves become qualitatively different as E_0 is changed. In particular, for $E_0 = 4.0$, the domain wall propagates smoothly, while increasing E_0 from $E_0 = 5.5$ to $E_0 = 6.5$ produces jerky motion, in which the domain wall slows dramatically for long-time intervals before breaking free again. Examination of Fig. 1 also shows that intervals of slow motion are strongly correlated with the presence of a large number of impurities on the domain wall, N, and vice versa. Transitions in domain wall speed are strongly correlated with a jump in the number of impurities on the domain wall.

It is instructive to consider how the changes in $R(t)$ are reflected in the distribution of the number of impurities on the domain wall $P(N)$, shown in Fig. 2, obtained from long-time simulations at several E_0. For relatively weak domain wall/impurity interactions ($E_0 = 5.25$), $P(N)$ is unimodal—the system is (almost always) in the fast regime. As the interaction strength is increased, $P(N)$ becomes bimodal as the system transits between the slow and fast regimes (i.e., jerky motion). Finally, for sufficiently strong interactions, $P(N)$ is again unimodal, with the system effectively trapped in the slow state.

In the jerky regime, observations of the system can be characterized by two distinct time scales, namely, t_S, the characteristic time that the domain wall motion remains slow (effectively trapped; many impurities on the domain wall) before it breaks free; and t_F, the characteristic time that the domain wall motion is fast (few impurities on the domain wall) before again being captured by the impurities. If our observation time t_O is smaller than both these

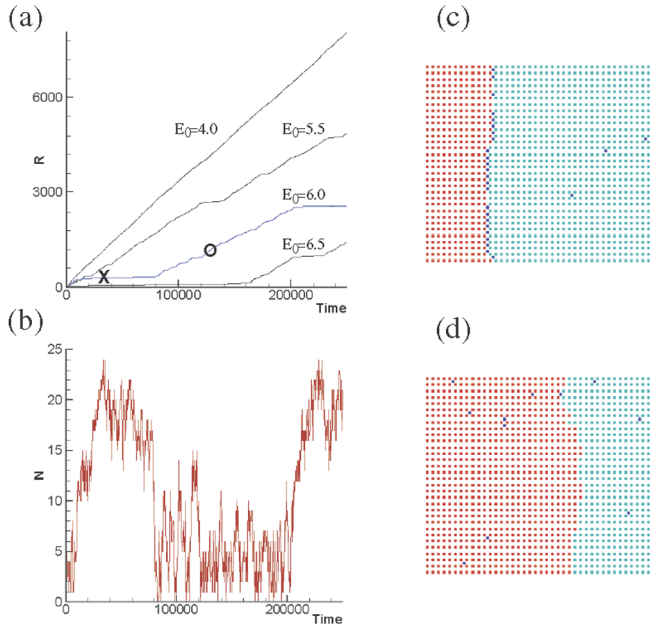

FIG. 1 (color online). (a) Position of the domain wall as a function of time for several values of the heat of segregation, E_0. (b) The number of impurities $N(t)$ on the domain wall, corresponding to the $E_0 = 6.0$ simulation in (a). (c),(d) Configurations of the domain wall and impurity positions at the times marked "X" and "O" in (a), respectively.

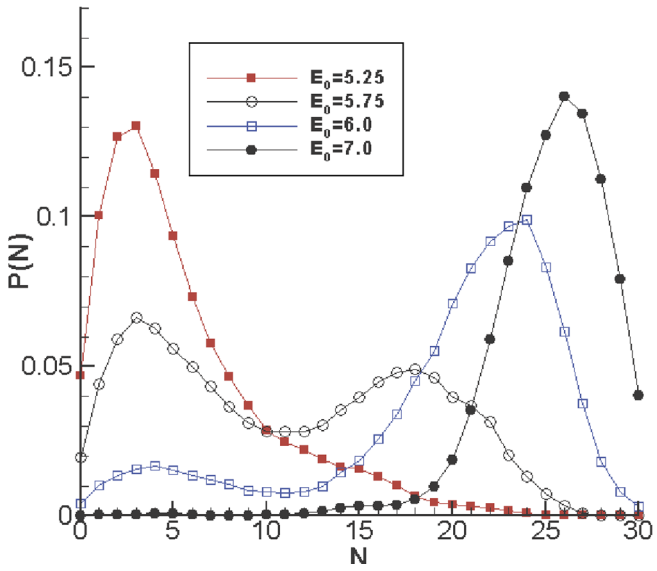

FIG. 2 (color online). Steady-state probability distributions $P(N)$ as a function of E_0, determined from long MC runs.

characteristic times, the system will *appear to us* in a typical simulation to be either only fast or only slow, depending on the initial condition (suggesting hysteresis). On the other hand, if t_O is much greater than these times, the domain wall appears to move at a constant speed that is an appropriately weighted average of the fast and slow speeds. The motion appears to be jerky only if t_O is in the range of the two characteristic times.

In what follows, we focus on the variable $N(t)$ and demonstrate that a quantitative description of the system can be developed based upon its dynamics. Assuming that $N(t)$ is an effective "slow variable" for the system, standard arguments based on the Mori-Zwanzig projection operator formalism (see, e.g., Ref. [10]) lead to a stochastic description of the system in terms of a Langevin equation for $N(t)$. Alternatively, we may consider a one-dimensional Fokker-Planck (FP) equation, describing the statistics of the stochastic motion of a "particle" in a two-well potential; here the particle corresponds to the instantaneous number of impurities on the domain wall $N(t)$, and the effects of all other degrees of freedom are incorporated into the effective potential. The effective FP equation for the corresponding probability distribution $P(N, t)$ is [11]

$$\frac{\partial P(N,t)}{\partial t} = \left[-\frac{\partial}{\partial N} V(N) + \frac{\partial^2 D(N)}{\partial N^2} \right] P(N,t), \qquad (1)$$

where $V(N) \equiv \lim_{\Delta t \to 0} \langle \Delta N \rangle / \Delta t$, $2D(N) \equiv \lim_{\Delta t \to 0} \langle [\Delta N]^2 \rangle / \Delta t$, and $\Delta N \equiv N(t + \Delta t) - N(t)$. At stationarity, $P(N) \propto \exp[-\Phi(N)/k_B T]$, where $\Phi(N)$ denotes the effective potential and is determined from V and D as

$$\frac{\Phi(N)}{k_B T} = \text{const.} - \int_0^N dN' \frac{V(N')}{D(N')} + \ln D(N). \qquad (2)$$

Note that, in the limit $D = \text{const.}$, Eq. (1) becomes equivalent to the Langevin equation $\frac{\partial N}{\partial t} = -\frac{D}{k_B T} \frac{d\Phi}{dN} + \eta$, where η is a random, stochastic variable that is Gaussian distributed with mean $\langle \eta \rangle = 0$ and variance $\langle \eta(t)\eta(s) \rangle = 2D\delta(t - s)$. Most importantly, our Monte Carlo (MC) simulations can be employed to extract both $V(N)$ and $D(N)$ "on demand" as follows: choose a value of N_0, locate several instances when it appears in a long-time simulation, tabulate the subsequent values of N within a fixed time interval Δt (here $\Delta t = 600$), and then average over these segments and estimate the rate of change in the mean (V) and the variance ($2D$) for the number of impurities on the domain wall. This is repeated for a grid of N_0 values sufficient to numerically evaluate the integral in Eq. (2) to the desired accuracy. Similar methods for estimating V and $2D$ from a stochastic time series have been presented in Refs. [12,13].

The result of this analysis is shown in Fig. 3, where we plot $\Phi(N)/k_B T$ for $E_0 = 6.0$ along with the potential obtained by directly constructing the probability distribution $P(N)$ from the time series and employing $P(N) \sim \exp(\Phi/k_B T)$. Indeed, $\Phi(N)/k_B T$ has a double-well structure, with minima at $N_F \approx 4$ and $N_S \approx 24$, and an (unstable) saddle transition point at $N_U = 11$. Furthermore, the effective potential extracted from the FP analysis shows good agreement with that obtained directly from the time series for $N > 6$. The discrepancy observed for small N can be rationalized by arguing that $\Phi(N)$ is no longer effectively one dimensional. In this regime, additional degrees of freedom, such as the domain wall shape, are no longer slaved to the single variable $N(t)$.

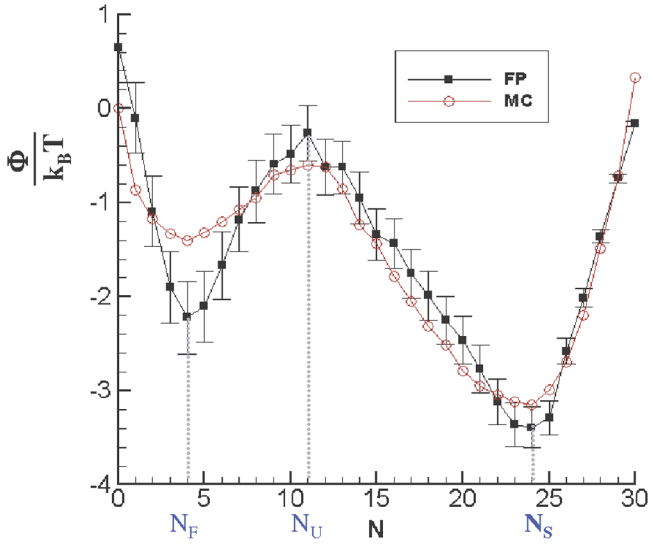

FIG. 3 (color online). The effective potential $\Phi(N)$ from Eq. (2) and directly from the long-time simulation data of Fig. 2 with $E_0 = 6.0$.

The form of the effective potential $\Phi(N)$ suggests that there is a single effective barrier or saddle that must be overcome for the system to move from the slow (pinned) state to the fast one (or vice versa). The waiting time between transitions between states depends on the shape of $\Phi(N)$ and the kinetic coefficient $D(N)$. Following Kramers (see, e.g., Ref. [14]), we can estimate this time τ as

$$\tau \approx \frac{2\pi k_B T}{\bar{D} \sqrt{\Phi''(N_{\min}) |\Phi''(N_{\text{saddle}})|}} e^{\Delta\Phi/k_B T}, \qquad (3)$$

where $2\bar{D} = D(N_{\min}) + D(N_{\text{saddle}})$. For the data represented in Fig. 3 corresponding to $E_0 = 6.0$, the average time needed for a transition from fast to slow and vice versa is $\tau \approx 4 \times 10^4$ and $\tau \approx 4 \times 10^5$, respectively. These are each within a factor of 3 of the waiting times estimated from a long MC simulation.

Armed with $\Phi(N)$ for several values of E_0, we now construct the domain wall speed vs impurity interaction strength, E_0, bifurcation diagram, as follows. We determine the average domain wall speed as a function of N, $\bar{V} = \bar{V}(N)$, for each E_0 from our numerical simulations. Then, we determine the velocity on the slow branch as

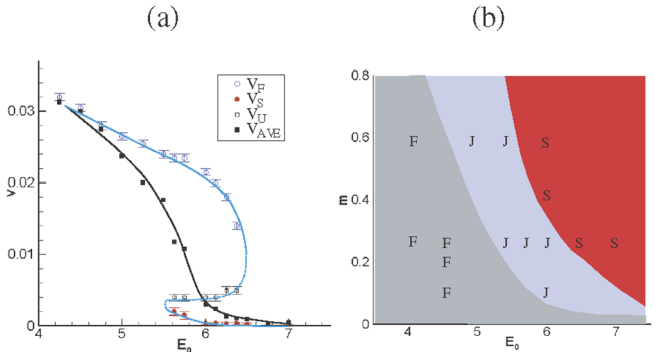

FIG. 4 (color online). (a) The effective domain wall velocity versus E_0 bifurcation diagram at $m = 0.25$. The solid and dotted lines are guides to the eye. (b) A diagram of the different regimes of behavior as a function of impurity mobility m and the impurity-domain wall interaction strength E_0; blue (light gray) denotes smooth, gray (dark gray) denotes jerky, and red (black) denotes effectively pinned propagation. Symbols are from measured data with "F" corresponding to fast, "J" to jerky, and "S" to slow (pinned) behavior, respectively.

$V_S = \bar{V}(N = N_S)$, on the fast branch as $V_F = \bar{V}(N = N_F)$, and on the unstable branch as $V_U = \bar{V}(N = N_U)$, where N_S, N_F, and N_U are from plots such as those in Figs. 2 and 3 for each value of E_0. The results are shown in Fig. 4, where we plot the stationary domain wall velocity vs interaction strength bifurcation diagram, including multiple stable branches and the unstable branch. Alternatively, we can search for the stationary values of N for which $dN/dt = 0$ using standard root-finding methods. dN/dt can be estimated as $\frac{N(t=t')-N(t=0)}{t'}$ by performing a series of short simulations initialized with $N(t = 0)$ impurities on the boundary for a time t' [13].

To summarize, we obtain both the stable and unstable branches of the bifurcation diagram, as well as an estimate of the characteristic time τ over which the domain wall will switch from fast to slow or vice versa. Therefore, hysteresis can be expected for observation times $t_O \ll \tau$, and the bifurcation diagram becomes single valued everywhere for observation times $t_O \gg \tau$. In the latter limit, the observed domain wall velocity will be $\bar{V}(E_0) = \int_0^\infty dN P(N; E_0)\bar{V}(N; E_0)$, as shown in Fig. 4. Increasing either the impurity diffusivity or the heat of segregation (or both) leads to more effective pinning and thus increasingly jerky domain wall dynamics. In Fig. 4 we show a morphological diagram for the propagation mode of the domain wall as a function of m and E_0 for $t_O = 10^4$. While we have applied this approach to domain wall motion in impure systems, it is directly applicable to hysteresis in a wide range of physical contexts. In all applications, the key is to determine the appropriate slow variables (domain wall-impurity concentration here).

Combining a coarse-grained computational approach with an *effective* Langevin/Fokker-Planck description for the stochastic dynamics of the impurity density along the domain wall provides a useful and computationally efficient method for determining the apparent stationary states (both stable and unstable) of the system, as well as for computing the transition rates between the stable states. The transition rates, together with the apparent stationary states, provide a clear picture of the dynamics of the coupled domain wall-impurity system and conditions for determining when hysteretic behavior will be observed. We believe that this approach can be used to quantify the emergence of hysteresis in a wide variety of physical systems. Whether hysteresis will be observed in a particular experiment or simulation depends, of course, on the physics. However, it does not only depend on the physics; it depends on the time scale of the observation and on the (length, ensemble) size of the system.

*Current address: Department of Materials Science and Engineering, McMaster University, 1280 Main Street West, Hamilton, Ontario, Canada L8S 4L7.
Electronic address: haataja@mcmaster.ca

[1] J.W. Cahn, Acta Metall. **10**, 789 (1962).
[2] G. Blatter *et al.*, Rev. Mod. Phys. **66**, 1125 (1994).
[3] P. Chauve, T. Giamarchi, and P. Le Doussal, Phys. Rev. B **62**, 6241 (2000).
[4] G. Grüner, Rev. Mod. Phys. **60**, 1129 (1988).
[5] P. Hähner *et al.*, Phys. Rev. B **65**, 134109 (2002).
[6] T. Tybell *et al.*, Phys. Rev. Lett. **89**, 097601 (2002).
[7] D. Cule and T. Hwa, Phys. Rev. Lett. **77**, 278 (1996).
[8] D. Maroudas and R. A. Brown, Appl. Phys. Lett. **58**, 1842 (1991).
[9] M. I. Mendelev, D. J. Srolovitz, and W. E, Philos. Mag. A **81**, 2243 (2001).
[10] D. Forster, *Hydrodynamic Fluctuations, Broken Symmetry, and Correlation Functions* (W. A. Benjamin, Inc., Reading, 1975).
[11] R. Kubo, M. Toda, and N. Hashitsume, *Statistical Physics II: Nonequilibrium Statistical Mechanics* (Springer-Verlag, Berlin, 1995), 2nd ed.
[12] J. Gradišek *et al.*, Phys. Rev. E **62**, 3146 (2000).
[13] G. Hummer and I. G. Kevrekidis, J. Chem. Phys.. **118**, 10762 (2003).
[14] P. Hänggi, P. Talkner, and M. Borkocev, Rev. Mod. Phys. **62**, 251 (1990).